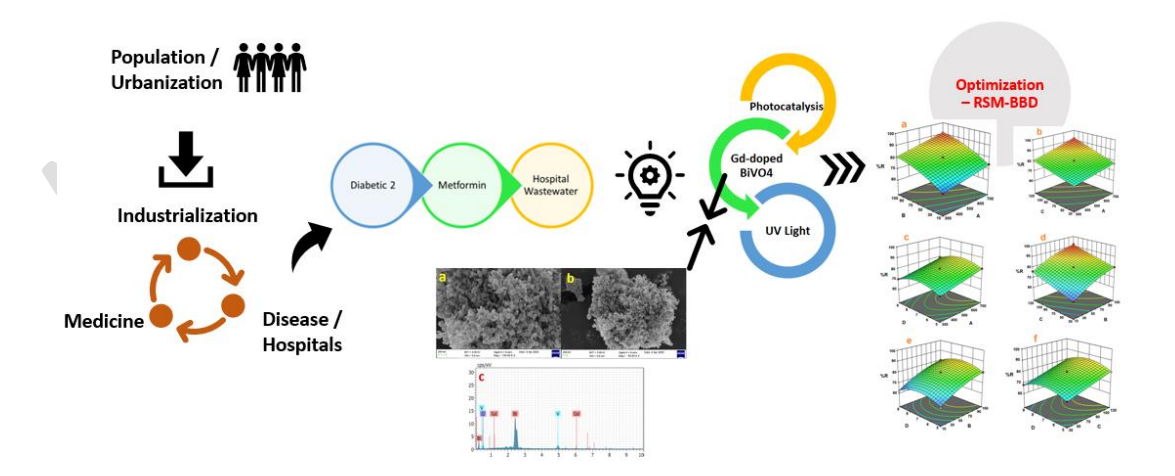
## Optimization of metformin removal by Gadolinium doped

- Bismuth Vanadate as photocatalyst in presence of
- 3 UV light source using Box-Behnken Design
- K. Murugesan<sup>a</sup>, N. Sivarajasekar<sup>b,\*</sup>, H. Arul<sup>c</sup>
- 5 a Department of Chemical Engineering, KPR Institute of Engineering and Technology, Coimbatore
- 6 *641407, India.*
- 7 b Laboratory for Bioremediation Research, Unit Operations Laboratory, Department of
- 8 Biotechnology, Kumaraguru College of Technology, Coimbatore 641 049, India.
- 11 \*Corresponding author.
- 12 E-mail address: sivarajasekar.n.bt@kct.ac.in (N. Sivarajasekar)

#### 13 Graphical abstract



1

## **ABSTRACT**

This study aimed to synthesize Gadolinium-doped Bismuth Vanadate (Gd-BV) using co-
precipitation and evaluate its effectiveness in removing metformin from metformin bearing
synthetic effluent and also optimization done using Response Surface Methodology (RSM),
specifically a Box-Behnken Design (BBD). A 5% Gd-doped BV photocatalyst was prepared
and tested for metformin removal under UV light source. The RSM-BBD approach,
implemented with DesignExpert software, explored the impact of initial metformin
concentration (300-700 mg L <sup>-1</sup> ), Gd-BV dosage (10-100 mg), reaction time (30-120 min), and
pH (5-9). The optimal conditions identified resulted in a 92% removal efficiency for
metformin, achieved with an initial concentration of 595.7 mg L <sup>-1</sup> , a catalyst dosage of 88.404
mg, a reaction time of 116 min, and a pH of 7.8.

*Keywords:* Metformin, Diabetes 2, Micropollutant, Water Treatment, Photocatalyst,
 Optimization, RSM-BBD, Statistical modelling, Bismuth Vanadate.

#### 31 1. INTRODUCTION

32

33

34

35

36

37

38

39

40

41

42

43

44

45

46

47

48

49

50

51

52

53

54

Metformin is used as diabetic type 2 medicine and threatens water pollution from hospital wastewater. Metformin causes environmental impact when release to the environment. It must be removed before release to water bodies. Photocatalysis is one of the prominent methods to remove metformin. Earlier, Titanium dioxide is used as photocatalyst, and recent days new materials are synthesized. Gadolinium doped Bismuth Vanadate is one of the good photocatalyst used recent days. Water is mandatory in all places. Nowadays industrial effluent treatment is the challengeable one. There are so many methods available to treat. Advanced oxidation process (AoP) is one of the efficient methods [1]. There are number of methods comes under AoP. Photocatalysis is one of the proven methods to treat the water. Metformin is one of the major threats to the environmental pollution. Following literatures review shows how metformin threatens the environment. According to the World Health Organization, the number of people diagnosed with diabetes is expected to exceed 350 million by the year 2030 [2]. Oral intake of metformin by human, an antidiabetic drug which is unmetabolized and 90% is removed in 12 hours via kidney and the remaining via faeces [2], [3], [4]. Metformin is the one of the highest consumed pharmaceuticals worldwide. Conventional methods such as activated carbon filtration and flocculation are not effective at removing metformin. The most effective removal method is chlorination, followed by ozonation, then activated carbon filtration, and finally flocculation, which is the least effective [5]. Sales data analysis taken in Ootmursum village and Enschede city (both at Netherland) showed that wastewater has the highest concentration of metformin (122.01 µg/L and 141.38 µg/L respectively) when compared to other drugs [6]. A study has indicated that metformin and amoxicillin are anticipated to be present in the environment at the

highest concentrations compared to other substances analysed [7]. Metformin affects the aqua life when it is released to the water bodies. It causes intersex and reduced fecundity in fish [8]. Photodegradation of metformin carried out using TiO<sub>2</sub> as photocatalyst. New photocatalysts are developed recent days and doping also will increase the efficiency [9]. Presence of metformin on sewage hospital wastewater, drinking water / drinking water treatment plant and surface water, concentrations on surface water has been reviewed [4]. By considering the impact of metformin to the environment, it is mandatory to treat the metformin from wastewater before release to the water bodies. Earlier days Titanium Dioxide was the mostly used photocatalyst [10]. Nowadays new photocatalyst are prepared as well as doped to bring more efficiency. Bismuth vanadate is one of the versatile photocatalyst used recent days and doping will enhance the efficiency. Rare earth ions ((RE=Ho, Sm, Yb, Eu, Gd, Nd, Ce and La) doped BiVO<sub>4</sub> found to be a prominent photocatalyst to organic matters. Among that Gadolinium doping results more efficient when compared to other rare earth dopants. It was found optimum concentration at Gd 10% by wt. [11]. Gd doped BiVO<sub>4</sub> has good crystallinity at near room temperature and degradation rate achieved up to 96% after 120 min at Gd 10% [12]. Lanthanum and Gadolinium doping with Bismuth Vanadate will decrease crystalline size and increase the surface area, leading to large increase in photocatalytic performance [13]. A gadolinium-doped bismuth vanadate (BiVO<sub>4</sub>) photocatalyst was successfully used to break down organic pollutants. When exposed to a UVA-LED light source, this catalyst achieved an impressive 98.3% decomposition of the pollutants within 120 minutes, with the optimal performance observed at a 4% gadolinium doping concentration. Bacterial inactivation also has been done [14]. When Gd (gadolinium) was present at concentrations of 4% to 6%, the material exhibited optimal photocatalytic efficiency. This process was powered by LED visible light, which served as an environmentally friendly light source. This study utilized BiVO4 doped with 5% Gadolinium (Gd), which was

55

56

57

58

59

60

61

62

63

64

65

66

67

68

69

70

71

72

73

74

75

76

77

78

- 80 chosen for its optimal concentration, exhibiting high reusability and stability over five
- 81 experimental runs [15].
- 82 Many studies discussed about undoped BiVO<sub>4</sub> [11], [12], [16], [13], [17], [15] and [18]. Band
- gap of undoped BiVO<sub>4</sub> is nearly 2.4 eV which is referred from previous study and Gd doped
- 84 BiVO<sub>4</sub> is 2.81 eV from current study.
- 85 Removal of metformin using Gd doped Bismuth Vanadate is not studied earlier. Novelty of
- 86 present work is the application of Gadolinium doped Bismuth Vanadate photocatalyst to
- 87 remove metformin from wastewater.
- 88 Table 1 (Annexure) shows that comprehensive review of photocatalyst material, catalyst
- 89 preparation, UV light sources, application of photocatalyst to treat the micropollutant,
- 90 micropollutant removal efficiency, optimal dopant percentage, reaction time, measure of
- 91 degradation.
- 92 Graphical abstract shows the overview of the current study.

#### 93 2. MATERIALS AND METHODS

#### **94 2.1. Materials**

99

- 95 Bismuth nitrate pentahydrate [Bi(NO<sub>3</sub>)<sub>3</sub>.5H<sub>2</sub>O 394.99 g/mol] purchased from Sigma Aldrich.
- Ammonium metavanadate (NH<sub>4</sub>VO<sub>3</sub> 116.98 g/mol) purchased from HiMedia Laboratories.
- 97 Gadolinium nitrate hexahydrate (GdNO<sub>3</sub>.6H<sub>2</sub>O 451.4 g/mol) purchased from SRL Chemical.
- 98 And required HNO<sub>3</sub> and NaOH (Sigma Aldrich) used for the synthesis.

#### 2.2 Experimental procedure

- 100 Mild Steel Research Heber Multi-Lamp Photo Reactor Single Wavelength, Model
- Name/Number: HML-LP88, Capacity: <1 KL, is used in the experimental study. Prepared
- nanomaterial is used to treat the synthesized pharma effluent. The following steps are involved

in the experimental part. UV light source of 125W lamps with 365 nm was used in the experiment [11]. Calculation for the number of photons emitted by a 125 W UV light source at 365 nm is given below.

#### Calculation of the energy of a single photon at 365 nm:

- The energy of a photon (E) is given by the formula:  $E = h c / \lambda$ , where, h (Planck's constant) =
- 108 6.626×10<sup>-34</sup> J·s; c (speed of light) =  $2.998\times10^8$  m/s;  $\lambda$  (wavelength) = 365 nm= $365\times10^{-9}$  m.
- 109 E=  $(6.626 \times 10^{-34} \text{ J} \cdot \text{s}) \times (2.998 \times 10^8 \text{ m/s}) / 365 \times 10^{-9} \text{ m}$
- 110  $E \approx 5.44 \times 10^{-19} \text{ J/photon}$

#### 111 Calculation of the number of photons per second:

- The power of the light source (125 W) represents the total energy emitted per second in Joules
- 113 (1 W = 1 J/s).

- Number of photons/second = Total Power (J/s) / Energy per photon (J/photon)
- Number of photons/second =  $125 \text{ J/s} / 5.44 \times 10^{-19} \text{ J/photon}$
- Number of photons/second  $\approx 2.29 \times 10^{20}$  photons/s
- Photon flux measured by ferrioxalate actinometry is 4.07 x 10<sup>-6</sup> einstein s<sup>-1</sup>.
- 1000 ppm of synthesised metformin effluent has been prepared. 1 ppm of metformin
  has been prepared using dilution method. Further different concentration of metformin can be
  prepared from the same mother solution. pH of the effluent kept at 7. Take 20 ml of the prepared
  300 ppm metformin in the beaker and 0.2 mg of 5% of Gd BV doped nanomaterial is added
  (10 mg for 1000 ml; 0.2 mg for 20 ml). Volume of the reactor for every run is maintained as
  20 ml. Before photo degradation, UV absorbance taken at zero min time. Then it is kept at UV
  photo-reactor. After 75 min, sample of degraded solution has been taken out and analysed using

UV spectroscopy absorbance test. The same has been repeated for Table 3 BBD Design. Negligible amount of metformin adsorption found in dark place (24 hrs test). Pollutant removal efficiency will be calculated using initial concentration (C<sub>o</sub>) and final concentration (C) as given in Equation (1):

129 % Degradation = 
$$(C_o-C)/C_o \times 100$$
 Eq. (1)

#### 2.2.1 Synthesis of Gd doped Bismuth Vanadate

Different methods available for the preparation of Gd-BV [11] [13], [14], [19]. Synthesis of Gd-BV is given below.

To prepare 0.2M Solution A, dissolve 2.42 grams of bismuth nitrate pentahydrate in 25 ml of water. Add 6 to 7 drops of concentrated nitric acid, then stir for 20 minutes. 0.58 g of Ammonium metavanadate is dissolved in 25 ml of water, stir well for 20 minutes and it is called as 0.2M Solution B. 4 g of NaOH pellet is dissolved in 50 ml of water to get 2M NaOH solution. Then add solution A and Solution B slowly with well stirring. The yellowish precipitate will be formed. Add NaOH solution drop by drop with continuous stirring. Stop adding NaOH when the pH reached 7. Keep the resultant solution for 24 hours with proper aluminium foil wrapped. Formed precipitate is Bismuth Vanadate (BV). Our aim is to dope Gd with BV. Next day, take the prepared content and add Gadolinium nitrate and then heat it in a water bath at 50 °C with continuous stirring. After one hour of heating as well as stirring, Gd is doped with BV. Keep it for 24 hours with aluminium foiled wrapper and filter it, wash three times with Deionized water and wash with ethyl alcohol once. Filtered wet powder is dried in hot air oven at 110 °C. After well dry, take the powder and grind it using agate mortar pestle and keep it in a muffle furnace at 400 °C. Calcined product is grinded again and the finished product is Gd doped Bismuth Vanadate.

#### 2.3 Characterization

X-ray diffraction (XRD) was performed using a Bruker D8 Advance instrument, employing a Cu K Alpha radiation source (1.5418 A° wavelength) at 40 kV and 30 mA. The scanning parameters were 0.3 s per step with a 0.02 degree increment. FTIR make is 'Bruker, Model: Alpha ECO-ATR'. Raman analysis carried out using Confocal Raman microscopy, WITec Germany, Alpha control 300RA. Manufactured by Zeiss and developed by Bruker Nano GmbH Berlin, Germany, this FESEM utilizes a high-tension 5kV field emission electron source and an in-lens secondary electron detector for detailed imaging. EDS make is Bruker. UV-DRS by UV - Jasco V-570 UV/VIS/NRI Spectrophotometer. BET Surface analysis by Quantachrome® ASiQwin<sup>TM</sup>, Quantachrome Instruments version 5.0.

#### 2.4 Experimental Design – Optimization Technique

Optimization study carried out by Response Surface Methodology - Box-Behnken Design (RSM-BBD) using Stat-Ease360 version of DesignExeprt software tool. Varying parameters are initial metformin concentration (300 mg L<sup>-1</sup> to 700 mg L<sup>-1</sup>), Gd-BV dosage (10 mg to100 mg), time taken for degradation (30 min to 120 min) and pH value (5-9); the measuring output is metformin removal efficiency (%R). Parameters and their range selection based on the previous study (Table 2 - Annexure). BBD Design is listed in the Table 3.

Table 3 BBD Design

Run	Initial Conc. mg L <sup>-1</sup>	Catalyst Dosage mg L <sup>-1</sup>	Degradation Time min.	pН	Removal efficiency %
1	500	55	30	9	68
2	700	55	75	5	80
3	700	100	75	7	91
4	500	55	120	9	80

5	500	55	75	7	80
6	500	100	120	7	92
7	700	55	75	9	79
8	500	10	75	9	62
9	300	100	75	7	80
10	500	55	75	7	80
11	300	55	30	7	70
12	500	55	30	5	69
13	500	10	120	7	76
14	500	10	30	7	63
15	500	100	30	7	80
16	500	55	75	7	80
17	500	55	75	7	80
18	300	10	75	7	65
19	700	55	120	7	92
20	500	100	75	9	80
21	500	55	75	7	80
22	500	100	75	5	80
23	300	55	120	7	80
24	300	55	75	5	70
25	300	55	75	9	70
26	500	55	120	5	80
27	700	10	75	7	74
28	500	10	75	5	63
29	700	55	30	7	77

RSM-BBD analysis is based on quadratic second order polynomial equation. Base formula used in ANOVA table is [20]:

171 
$$Y = \beta_o + \sum_{i=1}^k \beta_i x_i + \sum_{j=1}^k \beta_{ii} x_i^2 + \sum_{j< i=2}^k \beta_{ij} x_i x_j + \varepsilon$$
 Eq. (2)

In this equation, Y represents response; k means the number of the patterns; i and j are the index numbers for the pattern;  $\beta_0$  means intercept term;  $x_1, x_2...x_k$  are the coded independent variables;  $\beta_i$ ,  $\beta_{ii}$ ,  $\beta_{ij}$  are the first-order (linear)main effect; the quadratic (squared) effect; the interaction effect respectively; and the random error,  $\varepsilon$ , accounts for any differences or uncertainties when comparing predicted outcomes with actual measurements.

#### 3. RESULTS AND DISCUSSION

#### 3.1 Characterizations

#### 3.1.1. XRD Analysis

XRD pattern of Gd-BV 5% is shown in Figure. 1. The peak position matched with Bismuth Vanadate. Tetragonal Gd-BV structure was observed and the JCPDS card number is 04-012-7976. Peak position found at  $2\theta = 24.63$ , 28.22, 31.72, 34.58, 40.12, 45.63, 47.74, 54.65, 58.26 and 66.31. This XRD of GD-BV confirmed with references [12], [13], [14], [17], [15][18] and [21].

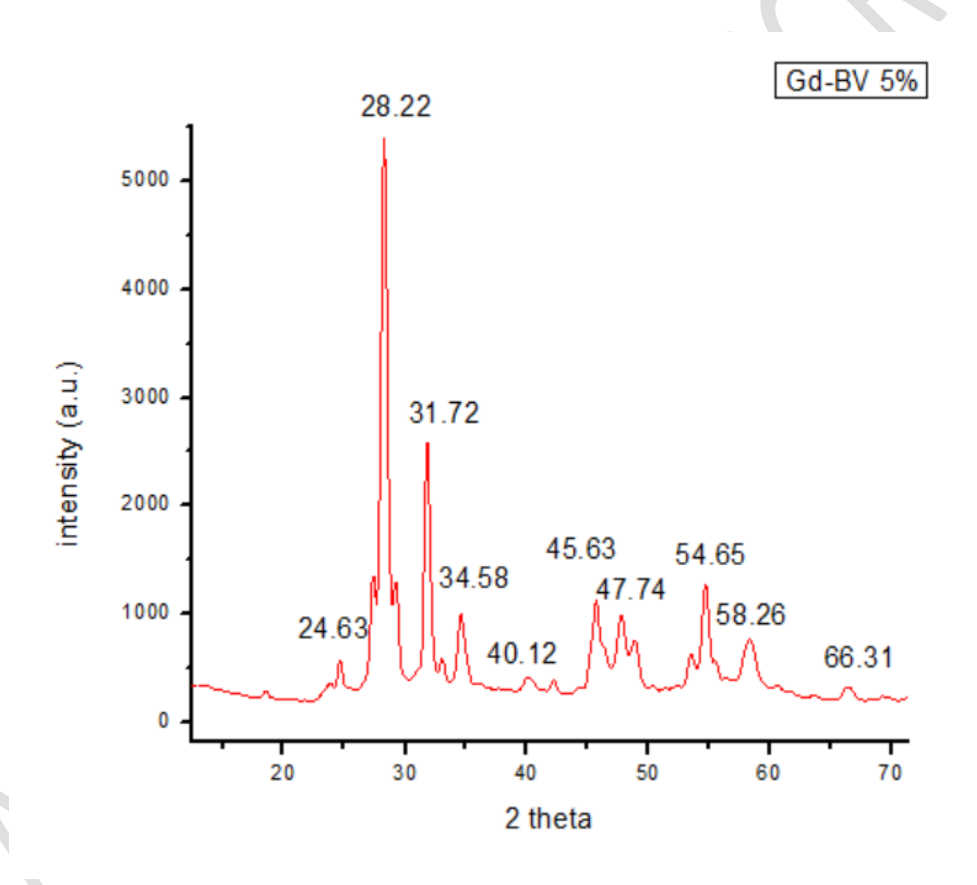


Figure. 1 XRD pattern of Gd-BV 5%

Scherrer formula  $D = K\lambda / \beta \cos\theta$ , is used to estimate the crystallite size (D) in nanometres.

K is the Scherrer constant, which is equal to 0.9

 $\lambda$  is the X-ray wavelength, is 0.15406 nm.

- $\beta$  is the full width at half maximum of the diffraction peak.
- $\theta$  is the peak position angle.

Calculated crystalline size is 98.83 nm.

#### 3.1.2. FTIR spectroscopy

FTIR taken for the prepared photocatalyst and reported in Figure 2. As per the standard value, obtained values are matched with VO4<sup>3-</sup>, Bi-O, V-O. Obtained peaks shows '% transmittance' corresponding to the wave number of 1363.96 cm<sup>-1</sup>, 736.93 cm<sup>-1</sup>, 520.46 cm<sup>-1</sup>. Gd-BV was well dried, so that trace of H-O-H bond does not exist. Clear peaks show there is no contamination. FTIR taken in the range of 500-2000 wavenumber. FTIR of GD-BV is fitted as per the previous studies [15], [22] and [18].

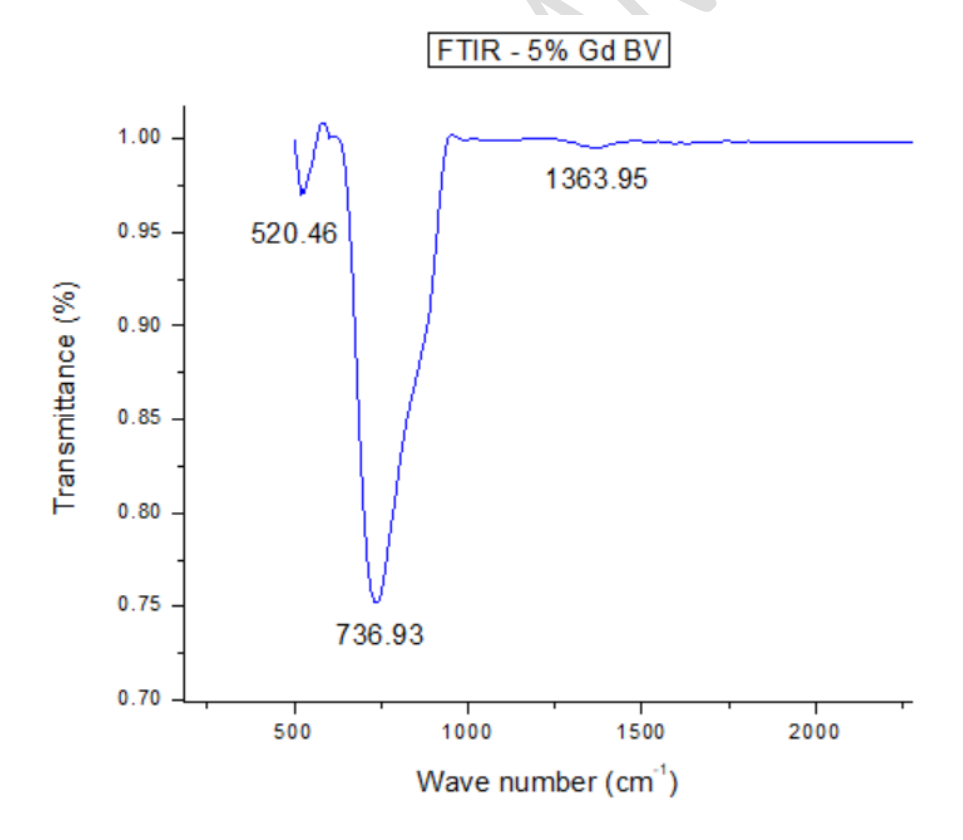


Figure. 2 FTIR of Gd-BV 5%

#### 3.1.3. Raman Spectroscopy

Figure 3 shows Raman analysis of prepared tetragonal Gd-BV nanomaterial. Molecular structure can be observed little more using Raman spectra. Peaks obtained at 850 cm<sup>-1</sup> wavenumber shows the V-O bond symmetric stretching mode and checked with the references [12], [17], [15] and [18]. Bi-O and O-V-O peaks are not clearly shown but the same is confirmed in FTIR analysis.

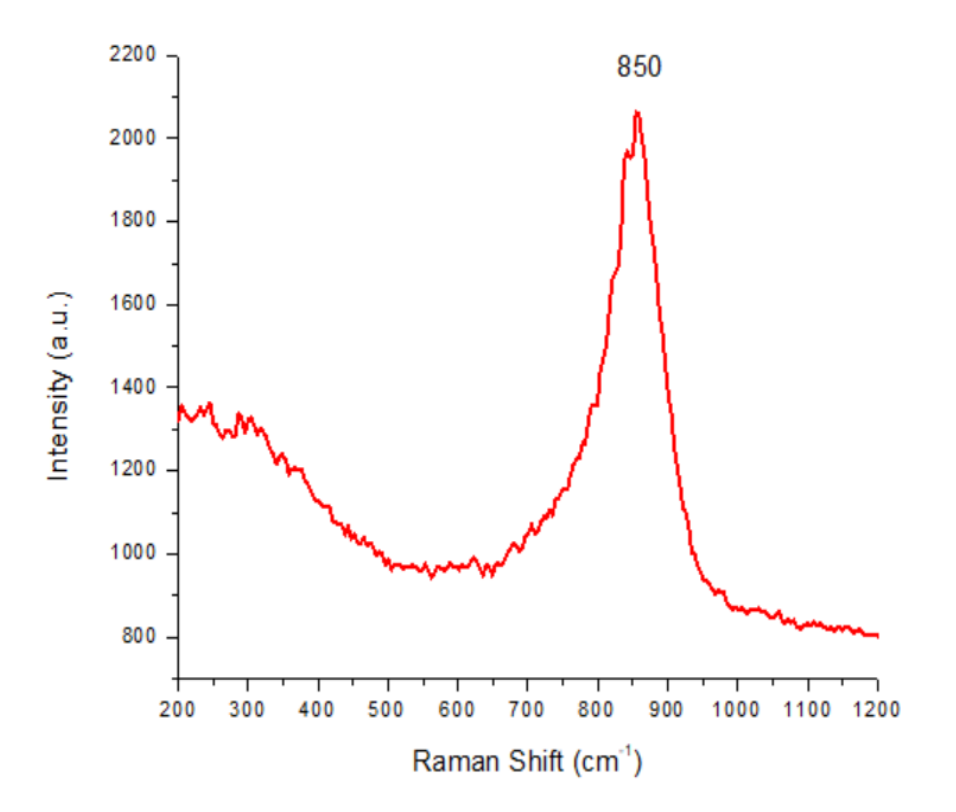


Figure. 3 Raman shift – Gd-BV 5%

#### 3.1.4. FE-SEM and EDS

Figure. 4a and 4b shows the surface morphology of Gd-BV as FE-SEM images. Figure. 4c shows EDS representation. Prepared nanomaterial shows spherical in shape [11], [14], [17], [15], [18] and having an average diameter of 100 nm which is calculated using XRD as 98.83 nm. It was observed that the elements Bi, V, O and Gd presents as per the EDS analysis and

matched with the references [12], [13], and [15]. Respective peaks of Bi, V, O and Gd are 2.525, 4.905, 0.550, 6.050 keV, respectively. EDS shows the purity of the material and homogenization.

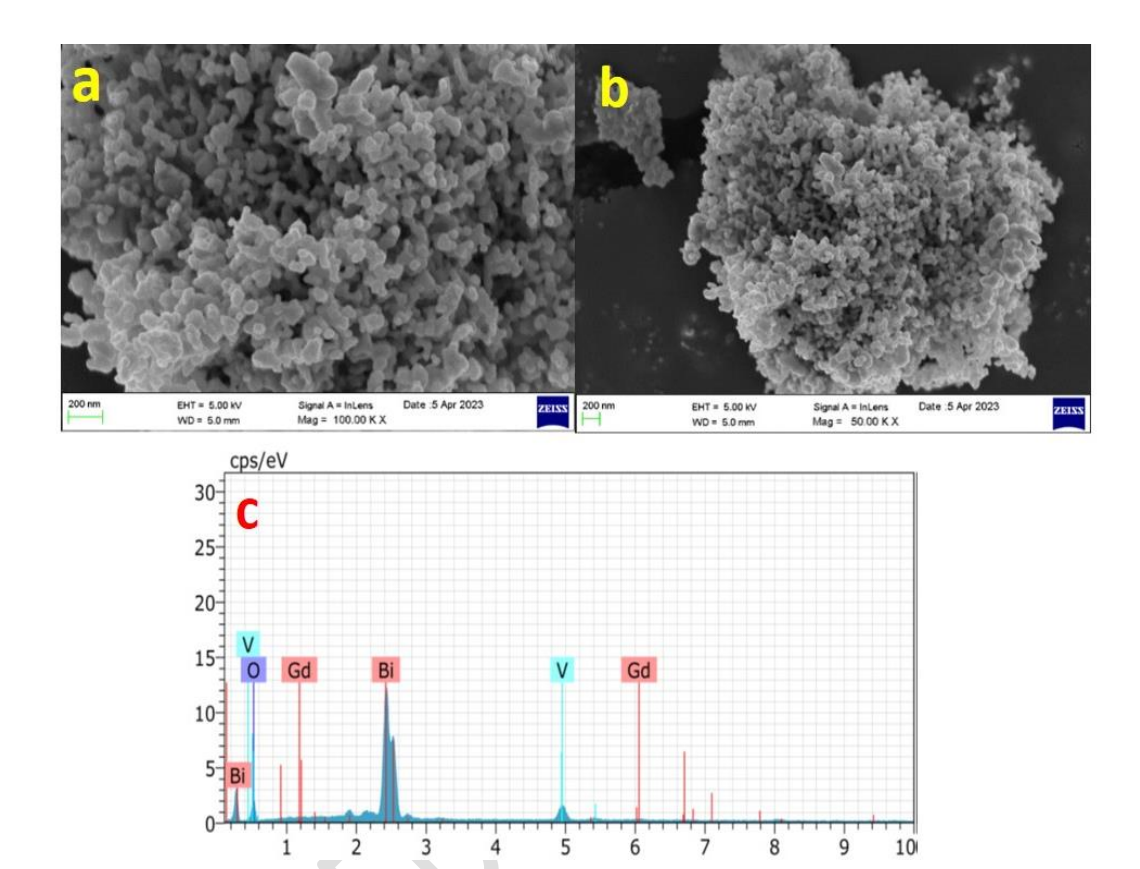


Figure. 4 (a) and (b) SEM Images (c) EDS analysis

## 3.1.5. UV-DRS Spectroscopy

UV-DRS analysis for the prepared nanomaterial powder GD-BV has been done. Figure. 5 shows the graphical representation between absorbance and bandgap energy. Band gap energy calculated as 2.81 eV using the Kubelka-Munk Function (KMF) with the help of equation 3. Obtained band gap energy is similar to the studies (Xu et al., 2009), [12], [14], [17], [15] and [18].

227 
$$KMF = F(R_{\infty}) = (1 - R_{\infty})^2 / 2R_{\infty} = K/S$$
 Eq. (3)

where,  $R_{\infty}$  represents the absolute reflectance of a material layer that is infinitely thick, K represents the absorption coefficient, while S represents the scattering coefficient.

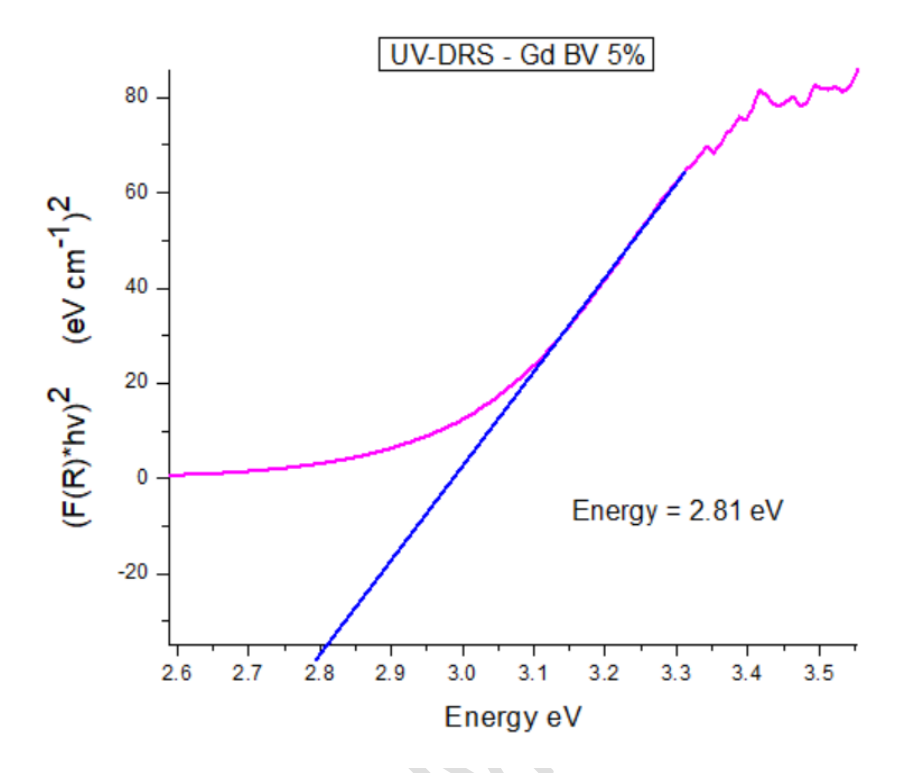


Figure. 5 UV-DRS analysis of 5% Gd-BV

#### 3.1.6. BET Surface area analysis

BET surface analysis has been done to know the specific surface area of Gd-BV which is shown in Figure. 6. Figure shows the adsorption and desorption plot between 'Volume at STP condition' and 'relative pressure P/P<sub>o</sub>'. Outgas time was 8.7 hrs; and outgas temperature was 250 °C. Nitrogen used for the analysis with a bath temperature of 77 K. Surface area determined from the analysis is 94.5 m<sup>2</sup>/g. Sample degassing at 150 °C and  $1.333 \times 10^{-4}$  Pa for 16 hours prior to the measurement. BET fitting range is found as 0.1 to 0.99 of relative pressure P/P°. BET summary is listed as, slope= 137.9 1/g; Intercept= 0.000e+00 1/g; Correlation coefficient, r = 1.0000000; C, constant= 0.708; Surface Area= 94.6 m<sup>2</sup>/g. BET surface area reported are [11]  $1.1 \text{ m}^2/\text{g}$ , [14] 8.7 m<sup>2</sup>/g, [15] 5-6 m<sup>2</sup>/g, [15] 11.9 m<sup>2</sup>/g, [22] 40.7 m<sup>2</sup>/g, and present work is 94.6

 $m^2/g$ . Pore volume and pore size determined by BJH (Barrett-Joyner-Halenda) is  $0.12 \text{ cm}^3/g$  and 3.5 nm respectively.

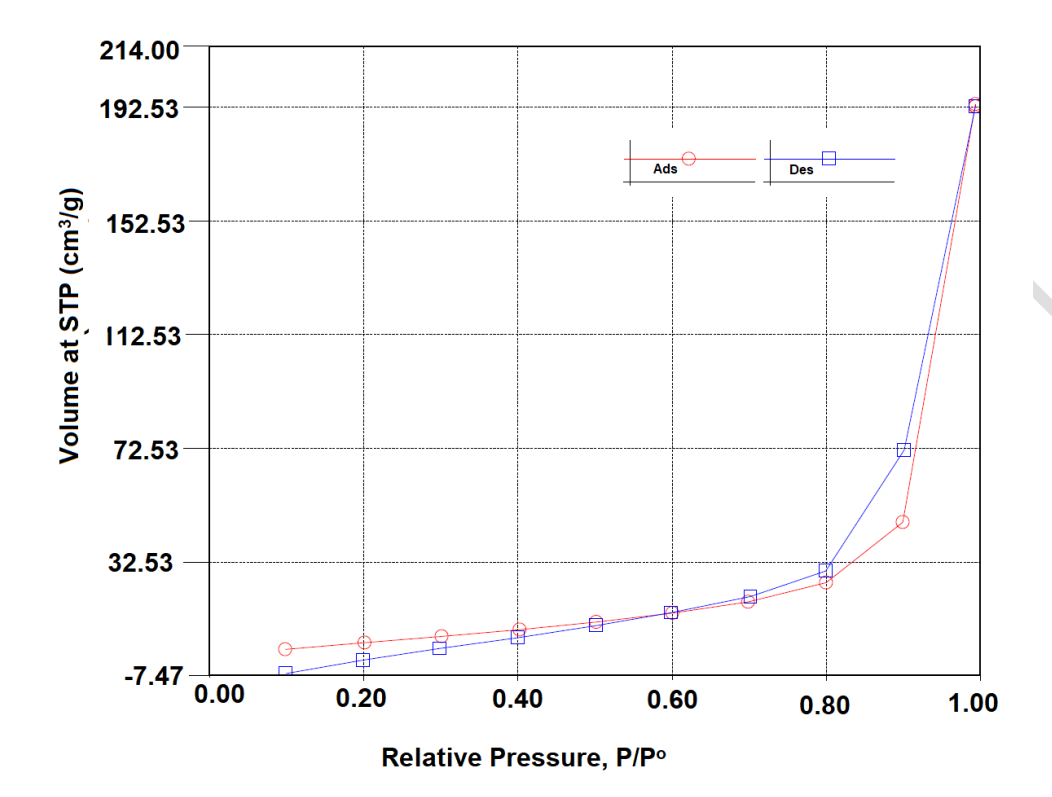


Figure. 6 BET – Linear Isotherm

#### 3.2 Proposed mechanism

- With reference to [15], [22], [18] and [23], mechanism of photocatalytic reaction steps is given below.
- i) UV light source emits photons.
- ii) When a photocatalyst called Gd-BV is exposed to UV-viz. light, electrons in its valence band (VB) get excited and jump to the conduction band (CB). This leaves an equal number of "holes" behind in the valence band.

253 iii) Photons fall on the surface of the semiconductor photocatalyst Gd-BV. Absorbed 254 photons are having energy (*hv*) greater than or equal to semiconductor band gap energy 255 (E<sub>BG</sub>).

256

257

258

259

260

261

262

263

264

265

266

267

268

269

276

- iv) When a material absorbs energy, it can create an electron-hole pair. This means an electron (e-) moves from the valence band (VB) to the conduction band (CB), leaving behind a "hole" (h+) in the valence band. Gd dopant will hinder the recombination and increase the efficiency.
  - v) When electrons interact with oxygen (O<sub>2</sub>) at the photocatalyst's surface, •O<sub>2</sub> superoxide radicals form, which are then transformed into •OH hydroxyl radicals.
  - vi) At the same time, holes results H<sub>2</sub>O into OH- and generate strong oxidizing agent •OH hydroxyl radicals which is the strong oxidizing agent.
- vii) •OH hydroxyl radicals reacts with organic matter and converted into CO<sub>2</sub> and H<sub>2</sub>O.
- viii) The incorporation of 5% Gadolinium (Gd) into Bismuth Vanadate (BiVO4) resulted in a band gap of 2.81 eV, determined by UV-DRS. This optimized band gap is expected to decrease electron-hole recombination, thereby boosting photocatalytic efficiency. Additionally, increased surface oxygen vacancies in the Gd-doped BiVO4 further facilitate the creation of electron-hole pairs.
- ix) With reference to [15], [22], [18], [18] and [23], proposed mechanism is given below.

Gd-BV + 
$$hv$$
 (UV light source)  $\rightarrow$  Gd-BV (h<sup>+</sup>) + Gd-BV (e<sup>-</sup>) Eq. (4)

272 Gd-BV (e<sup>-</sup>) + O<sub>2</sub> 
$$\rightarrow$$
 Gd-BV +  $\bullet$ O<sub>2</sub>- Eq. (5)

273 Gd-BV (h<sup>+</sup>) + H<sub>2</sub>O 
$$\rightarrow$$
 H<sup>+</sup> + OH<sup>-</sup> + Gd-BV Eq. (6)

274 Gd-BV (h<sup>+</sup>) + OH<sup>-</sup> 
$$\rightarrow$$
 •OH + Gd-BV Eq. (7)

Organic matter + •OH+ •O<sub>2</sub>-  $\rightarrow$  CO<sub>2</sub> + H<sub>2</sub>O + Degraded product Eq. (8)

Metformin can undergo both reduction and oxidation in a photocatalytic reaction and its reduction potential is around -0.5 V, and its oxidation potential is about +0.750 V. For a photocatalyst, the conduction band (where electrons accumulate after absorbing light) must be at a more negative energy level than the reduction potential of the molecule intended to gain electrons. This ensures that the photogenerated electrons have enough energy to reduce the adsorbed molecules. Conversely, the valence band (where "holes" are left after electrons move to the conduction band) needs to be at a more positive energy level than the oxidation potential of the molecule that will lose electrons. This allows the photogenerated holes to readily oxidize the adsorbed molecules.

- Band gap  $E_g = E_{CB}$  (conduction band potential) +  $E_{VB}$  (valance band potential)
- 287  $E_{CB} = X E_c 0.5 * E_g$
- where E<sub>c</sub> is the energy of free electrons on Hydrogen scale (4.5 eV) and X is the
- electronegativity (around 5.3 eV for Gd/BiVO<sub>4</sub>)

3.3 Kinetic Analysis and Metformin quantification

- 290  $E_{CB} = -0.605 \text{ eV}$ ;  $E_{VB} = +2.205 \text{ eV}$  which is valid for oxidation-reduction potential of
- 291 metformin.

277

278

279

280

281

282

283

284

285

292

- Plot between relative concentration 'ln(C/C<sub>o</sub>)' and degradation time 't' results the negative slope (rate constant 'k') and follows linear curve. So that it was concluded the kinetic model
- of pseudo-first order kinetics as follows.

297 
$$\ln(C/C_0) = -kt$$
 and  $C = C_0 e^{-kt}$  Eq. (9)

- where C represents the concentration remaining after the reaction, while C<sub>o</sub> is the initial concentration. Figure 7 shows plot between -lnC/Co vs time. Slope is 0.01355 and the intercept
- 300 is 0.00404.

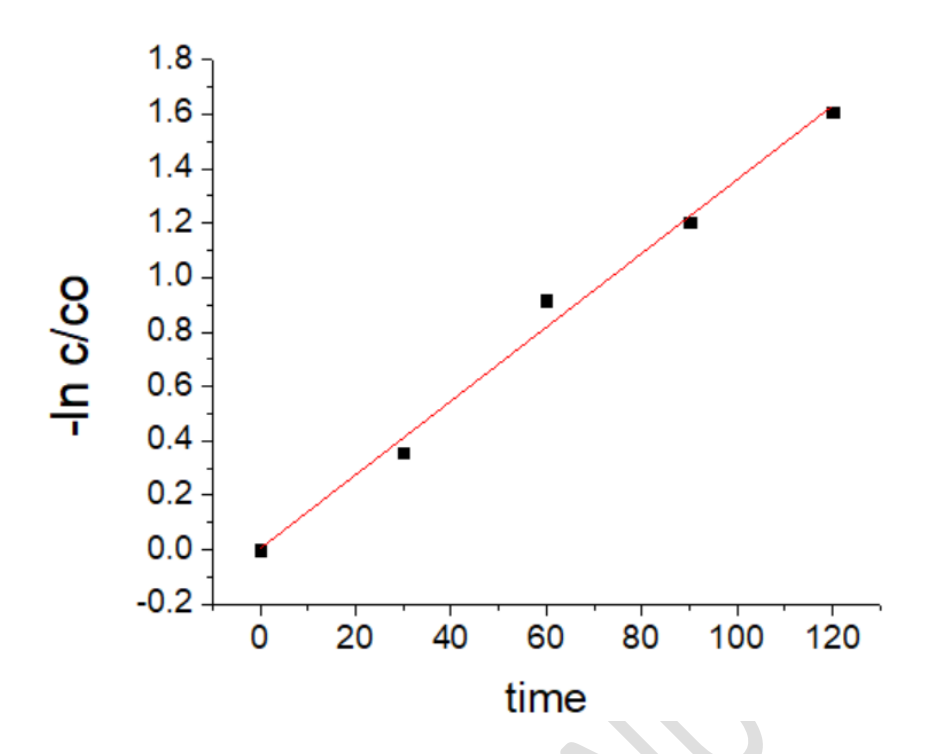


Figure 7. -lnC/C<sub>0</sub> vs. time

Metformin degradation was observed for each run using UV-spectroscopy which is shown in Figure 8a and 8b.

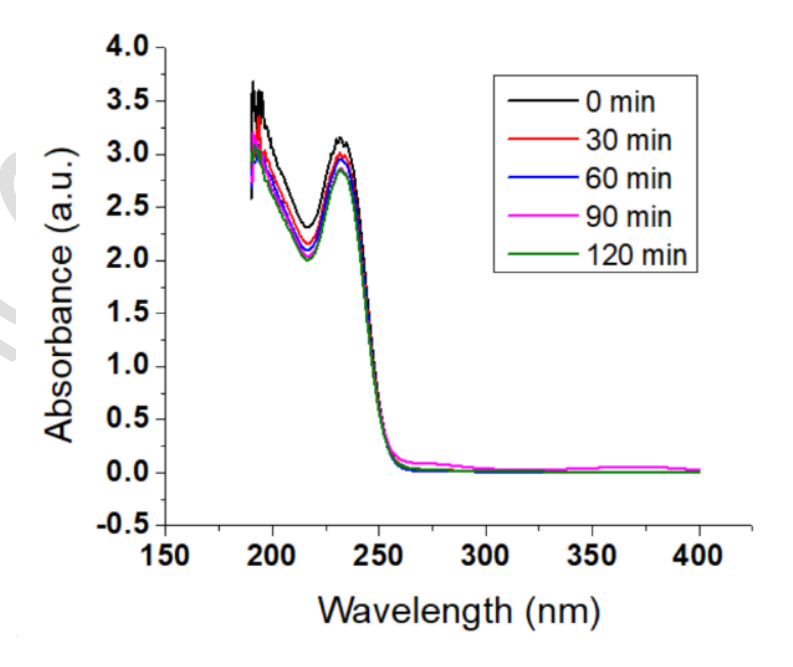


Figure. 8a – UV spectroscopy of Metformin degradation

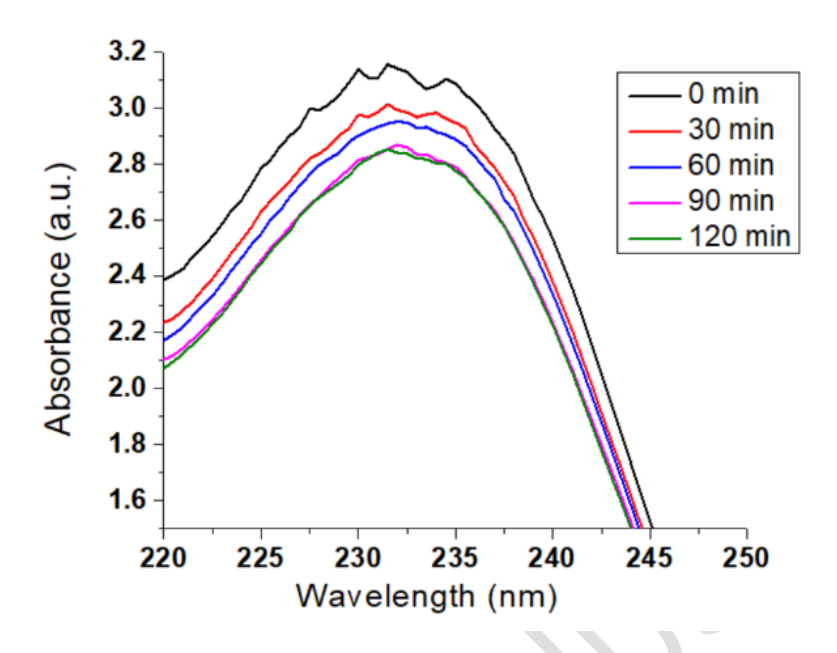


Figure. 8b – UV spectroscopy of Metformin degradation-enlarged view

## 3.4 Optimization Technique - RSM-BBD

From RSM BBD, Polynomial model is given in terms of Percentage Removal Efficiency (%R).

The coded equation is given in Equation (10)

313 
$$\%$$
**R** = 80.00 + 4.83 \* A + 8.33 \* B + 6.08 \* C + -0.25 \* D + 0.50 \* AB + 1.25 \* AC + -0.25

\* AD + 
$$-0.25$$
 \* BC +  $0.25$  \* BD +  $0.25$  \* CD +  $0.125$  \* A^2 +  $-2.625$  \* B^2 +  $-7.178$ \*10^-15

315 \* 
$$C^2 + -5.75 * D^2$$
 Eq. (10)

Varying parameters and metformin removal efficiency is shown in section 2.4, BBD Design - Table 3. RSM - BBD has been carried out and The chosen model uses the highest-degree polynomial possible, with all its extra terms proving statistically important, and without any hidden or misleading interactions. Table 4 shows the fit summary of the surface response analysis. Quadratic model has been suggested, adjusted R<sup>2</sup> value is 0.9953, predicted R<sup>2</sup> value

is 0.9866. The difference between adjusted  $R^2$  and predicted  $R^2$  must be less than 0.0087 which shows the model fits good.

The quadratic model, as presented in Table 5, is statistically significant with a p-value less than 0.0001. This is further supported by a Model F-value of 428.42, indicating the model is a strong predictor.

**Table 5 - ANOVA for Quadratic model** 

Source	Sum of Squares	df	Mean Square	F-value	p-value
Model	1820.78	14	130.06	428.42	< 0.0001
A-initial conc.	280.33	1	280.33	923.45	< 0.0001
B-cat. dosage	833.33	1	833.33	2745.10	< 0.0001
C-deg. time	444.08	1	444.08	1462.86	< 0.0001
D-pH	0.7500	1	0.7500	2.47	0.13
AB	1.00	1	1.00	3.29	0.09
AC	6.25	1	6.25	20.59	0.0005
AD	0.25	1	0.25	0.82	0.37
BC	0.25	1	0.25	0.82	0.37
BD	0.25	1	0.25	0.82	0.37
CD	0.25	1	0.25	0.82	0.37
A <sup>2</sup>	0.1014	1	0.10	0.33	0.57

B <sup>2</sup>	44.70	1	44.70	147.23	< 0.0001
C <sup>2</sup>	0.00	1	0.00	0.00	1.00
$D^2$	214.46	1	214.46	706.45	< 0.0001
Residual	4.25	14	0.30	Std. Dev.	0.55
Lack of Fit	4.25	10	0.42	R <sup>2</sup>	0.9977
Pure Error	0.00	4	0.00	Adj. R <sup>2</sup>	0.9953
Cor Total	1825.03	28	-	Pred. R <sup>2</sup>	0.9866
C.V. %	0.71	(		Adeq. Precision	74.65

328

329

330

331

332

The Predicted R<sup>2</sup> (0.9866) and Adjusted R<sup>2</sup> (0.9953) are quite close, with a difference less than 0.2, indicating good model agreement. Additionally, the Adequate Precision ratio of 74.6 is well above the desired minimum of 4, signifying a strong signal-to-noise ratio.

Resultant optimal removal efficiency of metformin is 92% at initial concentration of 596 mg L<sup>-1</sup>, catalyst dosage of 88 mg, running time of 116 min and pH value of 7.8.

333 Two factor ANOVA with replication provides the following result:

#### **ANOVA**

Columns 3769792 4 942448 1.3844 3.62E-54 2.462615 Interaction 86293.49 16 5393.343 1.667504 0.065553 1.745647 Within 323438 100 3234.38	71110 171						
Sample       25699.71       4       6424.928       1.986448       0.10233       2.462615         Columns       3769792       4       942448       1.3844       3.62E-54       2.462615         Interaction       86293.49       16       5393.343       1.667504       0.065553       1.745647         Within       323438       100       3234.38	Source of						
Columns 3769792 4 942448 1.3844 3.62E-54 2.462615 Interaction 86293.49 16 5393.343 1.667504 0.065553 1.745647 Within 323438 100 3234.38	Variation	SS	df	MS	F	P-value	F crit
Columns         3769792         4         942448         1.3844         3.62E-54         2.462615           Interaction         86293.49         16         5393.343         1.667504         0.065553         1.745647           Within         323438         100         3234.38	Sample	25699.71	4	6424.928	1.986448	0.10233	2.462615
Interaction 86293.49 16 5393.343 1.667504 0.065553 1.745647 Within 323438 100 3234.38	-				29		
Within 323438 100 3234.38	Columns	3769792	4	942448	1.3844	3.62E-54	2.462615
	Interaction	86293.49	16	5393.343	1.667504	0.065553	1.745647
Total 4205223 124	Within	323438	100	3234.38			
Total 4205223 124							
10111 7203223 127	Total	4205223	124				

Various plots from RSM - BBD is discussed as follows.

Model adequacy can be checked using Normal plot which is shown in figure 9. To confirm the regression model accurately represents the real system and doesn't violate any core assumptions, it needs to visualize the fitted model. This helps to verify if the model is a good fit. Specifically, the normality assumption is met if your residuals plot forms a roughly straight line [20].

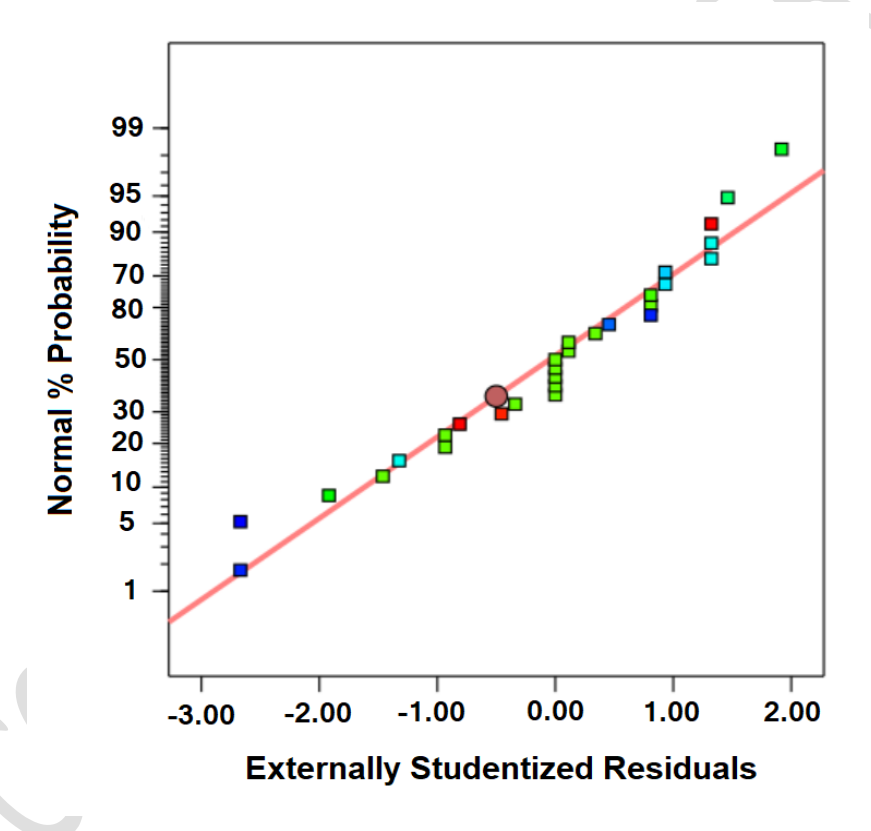


Figure. 9 Normal plot

Figure 10 displays a graph comparing the actual observed responses to the model's predicted values. The close alignment of these data points along a straight line (derived from a least squares fit) suggests the model accurately fits the data [20].

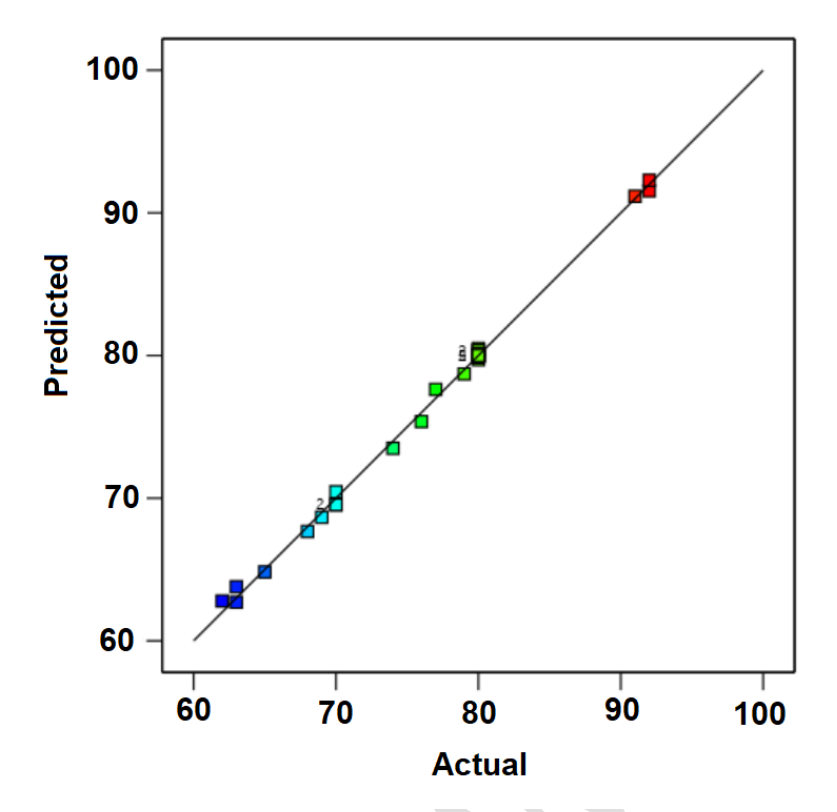


Figure. 10 Normal plot of residuals

#### 3.5. Effects of parameters and validation of the proposed model

3D plot can be drawn using RSM-BBD. It is very useful in the analysis of given problem. There are six plot list below in the figure 11a to f. Figure 11a, b, c speaks about initial concentration vs. other varying parameters. Figure shows, increase initial concentration will decrease the removal efficiency. Figure 11a, d, e speaks about catalyst dosage vs. other varying parameters. Metformin removal will increase when catalyst dosage increases. Figure 11c, e, f speaks about pH vs. other varying parameters. pH ranges from 5 to 9 taken for analysis. At lower pH and higher pH level, removal efficiency will decrease. Moderate pH range (near 7) will increase the removal efficiency. Figure 11b, d, f speaks about degradation time vs. other varying parameters. When degradation time increases, removal efficiency also will increase.

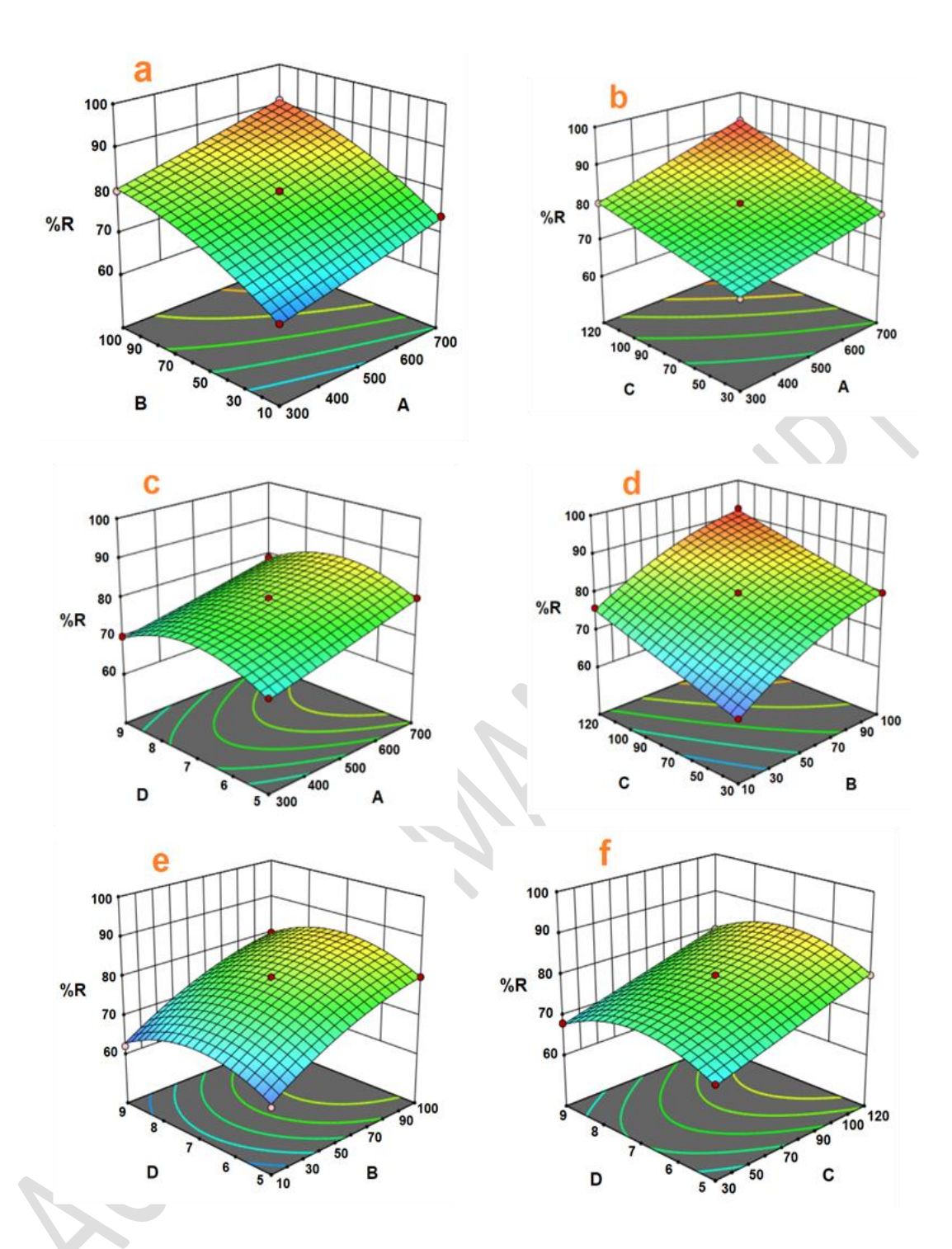


Figure. 11a to f - RSM-BBD 3D plot; A – initial concentration (mg  $L^{-1}$ ); B – Catalyst Dosage (mg  $L^{-1}$ ); C – Degradation time (min.); D – pH

The optimal solution found from the RSM-BBD (experimental values given in bracket) is given as initial concentration 596 mg L<sup>-1</sup> (exp: 596 mg L<sup>-1</sup>) catalyst dosage 88 mg (exp: 596

mg), degradation time 116 min (exp: 115 min), pH 7.8 (exp: 7.8) and removal efficiency 92.2% (exp: 92.5%)

#### 3.6 Metformin degradation – comparison

Table 6. Metformin degradation: current study vs. previous studies

Method	Catalyst	% F.cc:	Reference
	used	Efficiency	
Biodegradation	-	48.7	[3]
Membrane bioreactor	-	90	[24,25]
Photocatalysis – UV irradiation, 365 nm	TiO <sub>2</sub>	90	[26]
Hybrid Vertical Anaerobic Biofilm-	-	77	[27]
Reactor (HyVAB)			
TiO2-ZrO2 photocatalysis under UV	TiO2-ZrO2	100	[4]
radiation – toxicity test performed			
Photocatalysis – UV irradiation, 365 nm	Gd-BiVO <sub>4</sub>	92	Current study

## 3.7 Optimization using Genetic Algorithm

Genetic algorithm is an AI based optimization tool which is based on the earlier Darwin theory. After feeding our data (encoding), It will select randomly the individual population, and create the new population via crossover / mutation, and evaluated called offspring, then gives solution. In case of no optimal solution at this step, again select the random population and the step is repeated.

MATLAB GA toolbox was used to run the algorithm and the result is: Global optimal values for metformin removal found at initial concentration of 601 mg L<sup>-1</sup>, catalyst dosage of 84 mg, running time of 120 min and pH value of 7.8.

## 3.8 Reusability of catalyst

Prepared nanomaterial Gd-BV was used for 120 min. of experiment. Reusability test was performed and the same is shown in figure 12. The adsorption capacity was decreased  $\pm 7\%$  for each cycle of experiment and gradually deactivated. It could be reused for five times. Desorption can be done using diluted NaOH (1 N) is used to bring the higher generation capacity because of OH- ions presence.

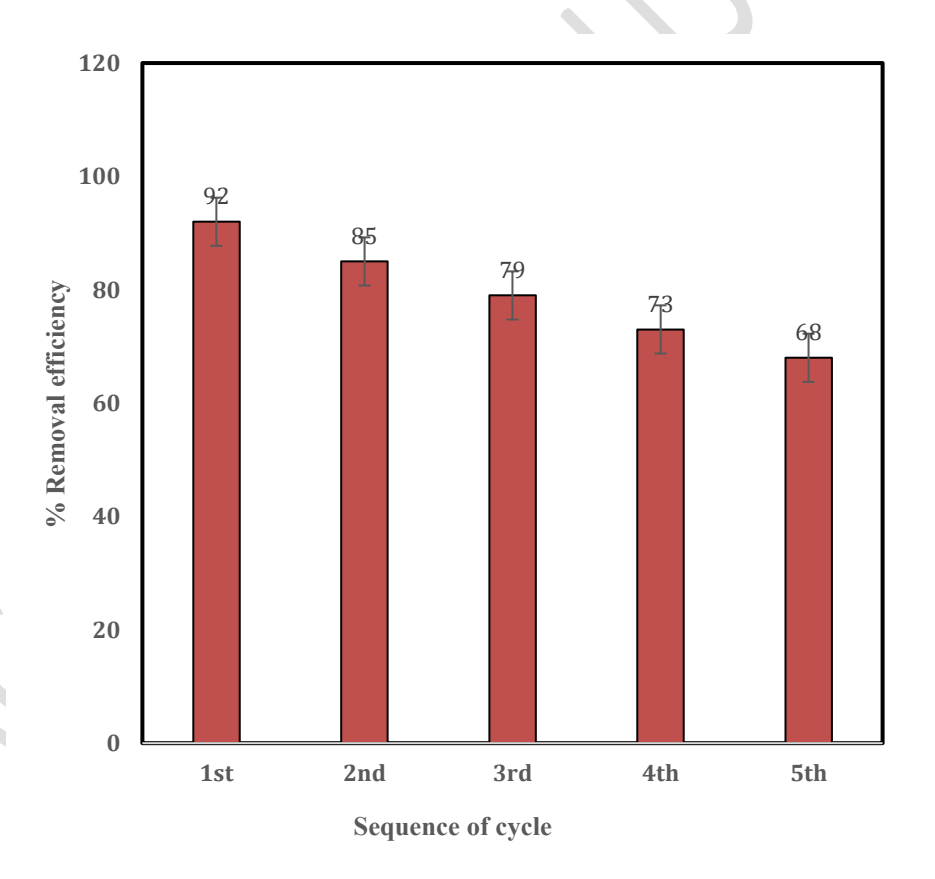


Figure. 12 %R vs. sequence of cycle

#### 4. CONCLUSION

388

Photocatalytic degradation of metformin has been done using Gadolinium doped Bismuth 389 Vanadate in presence of UV light source. Gd doped BiVO<sub>4</sub> is prepared using co-precipitation 390 method and the characterization methods XRD, FTIR, Raman Spectra, FE-SEM, EDS, UV-391 DRS and BET surface analysis confirmed the prepared nanomaterial is fit to the required 392 characteristics. Response Surface Methodology – Box-Behnken Design carried out using Stat-393 Ease 360 version of DesignExpert statistical software tool. Varying parameters, initial 394 concentration of metformin, catalyst dosage, degradation time and pH are analysed and the 395 resultant optimal removal efficiency of metformin is 92 % at initial concentration of 596 mg 396 L<sup>-1</sup>, catalyst dosage of 88 mg, running time of 116 min and pH value of 7.8. Also, the 397 optimization has been done using Genetic algorithm tool and optimal global values was found. 398 There are less studies available for are earth materials doped with BiVO<sub>4</sub>. There is a future 399 scope to dope with other rare earth materials and use it for photodegradation. 400

#### 5. REFERENCES

- K.T. Drisya, M. Solís-López, J.J. Ríos-Ramírez, J.C. Durán-Álvarez, A. Rousseau, S.
   Velumani, R. Asomoza, A. Kassiba, A. Jantrania, H. Castaneda, Electronic and optical
   competence of TiO2/BiVO4 nanocomposites in the photocatalytic processes, Sci Rep 10
   (2020). https://doi.org/10.1038/s41598-020-69032-9.
- 406 [2] C. Trautwein, J.D. Berset, H. Wolschke, K. Kümmerer, Occurrence of the antidiabetic drug
  407 Metformin and its ultimate transformation product Guanylurea in several compartments of the
  408 aquatic cycle, Environ Int 70 (2014) 203–212. https://doi.org/10.1016/j.envint.2014.05.008.
- 409 [3] C. Trautwein, K. Kümmerer, Incomplete aerobic degradation of the antidiabetic drug
  410 Metformin and identification of the bacterial dead-end transformation product Guanylurea,
  411 Chemosphere 85 (2011) 765–773. https://doi.org/10.1016/j.chemosphere.2011.06.057.
- 412 [4] C.F. Carbuloni, J.E. Savoia, J.S.P. Santos, C.A.A. Pereira, R.G. Marques, V.A.S. Ribeiro,
   413 A.M. Ferrari, Degradation of metformin in water by TiO2–ZrO2 photocatalysis, J Environ
   414 Manage 262 (2020). https://doi.org/10.1016/j.jenvman.2020.110347.
- 415 [5] M. Scheurer, A. Michel, H.J. Brauch, W. Ruck, F. Sacher, Occurrence and fate of the
  416 antidiabetic drug metformin and its metabolite guanylurea in the environment and during
  417 drinking water treatment, Water Res 46 (2012) 4790–4802.
  418 https://doi.org/10.1016/j.watres.2012.06.019.

- 419 [6] M. Oosterhuis, F. Sacher, T.L. ter Laak, Prediction of concentration levels of metformin and 420 other high consumption pharmaceuticals in wastewater and regional surface water based on 421 sales data, Science of the Total Environment 442 (2013) 380–388. 422 https://doi.org/10.1016/j.scitotenv.2012.10.046.
- F. Mansour, M. Al-Hindi, W. Saad, D. Salam, Environmental risk analysis and prioritization of pharmaceuticals in a developing world context, Science of the Total Environment 557–558 (2016) 31–43. https://doi.org/10.1016/j.scitotenv.2016.03.023.
- 426 [8] N.J. Niemuth, R.D. Klaper, Emerging wastewater contaminant metformin causes intersex and 427 reduced fecundity in fish, Chemosphere 135 (2015) 38–45. 428 https://doi.org/10.1016/j.chemosphere.2015.03.060.
- P. Chinnaiyan, S.G. Thampi, M. Kumar, M. Balachandran, Photocatalytic degradation of metformin and amoxicillin in synthetic hospital wastewater: effect of classical parameters, International Journal of Environmental Science and Technology 16 (2019) 5463–5474. https://doi.org/10.1007/s13762-018-1935-0.
- T. Saison, N. Chemin, C. Chanéac, O. Durupthy, L. Mariey, F. Maugé, V. Brezová, J.P.
   Jolivet, New insights into BiVO4 properties as visible light photocatalyst, Journal of Physical
   Chemistry C 119 (2015) 12967–12977. https://doi.org/10.1021/acs.jpcc.5b01468.
- H. Xu, C. Wu, H. Li, J. Chu, G. Sun, Y. Xu, Y. Yan, Synthesis, characterization and
   photocatalytic activities of rare earth-loaded BiVO 4 catalysts, Appl Surf Sci 256 (2009) 597–
   602. https://doi.org/10.1016/j.apsusc.2009.05.102.
- 439 [12] Y. Luo, G. Tan, G. Dong, H. Ren, A. Xia, A comprehensive investigation of tetragonal Gd-440 doped BiVO 4 with enhanced photocatalytic performance under sun-light, Appl Surf Sci 364 441 (2016) 156–165. https://doi.org/10.1016/j.apsusc.2015.12.100.
- J. Jia, M. Zhang, Z. Liu, C. Yu, W. Zhou, Z. Li, La3+,Gd3+-codoped BiVO4 nanorods with superior visible-light-driven photocatalytic performance for simultaneous removing aqueous Cr(VI) and azo dye, Journal of Nanoparticle Research 22 (2020). https://doi.org/10.1007/s11051-020-05012-4.
- C. Orona-Návar, I. Levchuk, J. Moreno-Andrés, Y. Park, A. Mikola, J. Mahlknecht, M.
   Sillanpää, N. Ornelas-Soto, Removal of pharmaceutically active compounds (PhACs) and
   bacteria inactivation from urban wastewater effluents by UVA-LED photocatalysis with Gd3+
   doped BiVO4, J Environ Chem Eng 8 (2020). https://doi.org/10.1016/j.jece.2020.104540.
- 450 [15] H. Abdelraouf, J. Ding, J. Ren, G. Zhao, F. Zhou, S. Guan, X. Zhai, Q. Zhao, Gd-BiVO4 451 photocatalyst for organic contaminants removal: Short-term synthesis at sub-100 °C and 452 enhanced sunlight-driven photocatalytic activity, Process Safety and Environmental Protection 453 168 (2022) 892–906. https://doi.org/10.1016/j.psep.2022.10.069.
- 454 [16] S.D. Dolić, D.J. Jovanović, K. Smits, B. Babić, M. Marinović-Cincović, S. Porobić, M.D.
   455 Dramićanin, A comparative study of photocatalytically active nanocrystalline tetragonal
   456 zyrcon-type and monoclinic scheelite-type bismuth vanadate, Ceram Int 44 (2018) 17953–
   457 17961. https://doi.org/10.1016/j.ceramint.2018.06.272.
- C. Orona-Návar, Y. Park, V. Srivastava, N. Hernández, J. Mahlknecht, M. Sillanpää, N.
   Ornelas-Soto, Gd3+ doped BiVO4 and visible light-emitting diodes (LED) for photocatalytic decomposition of bisphenol A, bisphenol S and bisphenol AF in water, J Environ Chem Eng 9 (2021). https://doi.org/10.1016/j.jece.2021.105842.

- 462 [18] M. Noor, F. Sharmin, M.A.A. Mamun, S. Hasan, M.A. Hakim, M.A. Basith, Effect of Gd and
   463 Y co-doping in BiVO4 photocatalyst for enhanced degradation of methylene blue dye, J
   464 Alloys Compd 895 (2022). https://doi.org/10.1016/j.jallcom.2021.162639.
- 465 [19] M. Wang, Y. Che, C. Niu, M. Dang, D. Dong, Effective visible light-active boron and 466 europium co-doped BiVO4 synthesized by sol-gel method for photodegradion of methyl 467 orange, J Hazard Mater 262 (2013) 447–455. https://doi.org/10.1016/j.jhazmat.2013.08.063.
- 468 [20] D.C.M.C.M.A.-C. Raymond H. Myers, RESPONSE SURFACE METHODOLOGY, 2016.
- J. Sun, Z. Wang, H. Lu, W. Zhang, Selective site doping impact on the phase transition in bismuth vanadate, Mater Lett 330 (2023). https://doi.org/10.1016/j.matlet.2022.133358.
- 5. Bashir, A. Jamil, M.S. Khan, A. Alazmi, F.A. Abuilaiwi, M. Shahid, Gd-doped BiVO4 microstructure and its composite with a flat carbonaceous matrix to boost photocatalytic performance, J Alloys Compd 913 (2022). https://doi.org/10.1016/j.jallcom.2022.165214.
- 474 [23] M.M. Sajid, N. Amin, N.A. Shad, S.B. khan, Y. Javed, Z. Zhang, Hydrothermal fabrication of monoclinic bismuth vanadate (m-BiVO4) nanoparticles for photocatalytic degradation of toxic organic dyes, Materials Science and Engineering: B 242 (2019) 83–89.

  477 https://doi.org/10.1016/j.mseb.2019.03.012.
- V.S. Kumar, M. Dhivakar, S. Nagamani, A. Dhanalakshmi, M.A. Leema, Removal of
   pharmaceuticals from wastewater: a review of different adsorptive approaches, Global Nest
   Journal 26 (2024). https://doi.org/10.30955/gnj.005300.
- 481 [25] M. Kim, P. Guerra, A. Shah, M. Parsa, M. Alaee, S.A. Smyth, Removal of pharmaceuticals 482 and personal care products in a membrane bioreactor wastewater treatment plant, Water 483 Science and Technology 69 (2014) 2221–2229. https://doi.org/10.2166/wst.2014.145.
- P. Chinnaiyan, S.G. Thampi, M. Kumar, M. Balachandran, Photocatalytic degradation of metformin and amoxicillin in synthetic hospital wastewater: effect of classical parameters, International Journal of Environmental Science and Technology 16 (2019) 5463–5474. https://doi.org/10.1007/s13762-018-1935-0.
- 488 [27] E. Janka, D. Carvajal, S. Wang, R. Bakke, C. Dinamarca, Treatment of metformin-containing 489 wastewater by a hybrid vertical anaerobic biofilm-reactor (HyVAB), Int J Environ Res Public 490 Health 16 (2019). https://doi.org/10.3390/ijerph16214125.
- 491 [28] K. Balasubramani, N. Sivarajasekar, M. Naushad, Effective adsorption of antidiabetic
   492 pharmaceutical (metformin) from aqueous medium using graphene oxide nanoparticles:
   493 Equilibrium and statistical modelling, J Mol Liq 301 (2020).
   494 https://doi.org/10.1016/j.molliq.2019.112426.
- T. Suresh, N. Sivarajasekar, K. Balasubramani, T. Ahamad, M. Alam, M. Naushad, Process intensification and comparison of bioethanol production from food industry waste (potatoes) by ultrasonic assisted acid hydrolysis and enzymatic hydrolysis: Statistical modelling and optimization, Biomass Bioenergy 142 (2020) 105752.

  https://doi.org/10.1016/j.biombioe.2020.105752.
- [30] N. Sivarajasekar, N. Mohanraj, S. Sivamani, J. Prakash Maran, I. Ganesh Moorthy, K.
   Balasubramani, Statistical optimization studies on adsorption of ibuprofen onto Albizialebbeck
   seed pods activated carbon prepared using microwave irradiation, in: Mater Today Proc,
   Elsevier Ltd, 2018: pp. 7264–7274. https://doi.org/10.1016/j.matpr.2017.11.394.

504 [31] N. Chaibakhsh, N. Ahmadi, M.A. Zanjanchi, Optimization of photocatalytic degradation of neutral red dye using TiO2 nanocatalyst via Box-Behnken design, Desalination Water Treat 57 505 (2016) 9296–9306. https://doi.org/10.1080/19443994.2015.1030705. 506 N. Tafreshi, S. Sharifnia, S. Moradi Dehaghi, Box-Behnken experimental design for 507 [32] optimization of ammonia photocatalytic degradation by ZnO/Oak charcoal composite, Process 508 Safety and Environmental Protection 106 (2017) 203–210. 509 https://doi.org/10.1016/j.psep.2017.01.015. 510 E. Bazrafshan, T.J. Al-Musawi, M.F. Silva, A.H. Panahi, M. Havangi, F.K. Mostafapur, 511 [33] Photocatalytic degradation of catechol using ZnO nanoparticles as catalyst: Optimizing the 512 experimental parameters using the Box-Behnken statistical methodology and kinetic studies, 513 Microchemical Journal 147 (2019) 643–653. https://doi.org/10.1016/j.microc.2019.03.078. 514 M. Assassi, F. Madjene, S. Harchouche, H. Boulfiza, Photocatalytic treatment of Crystal 515 [34] Violet in aqueous solution: Box-Behnken optimization and degradation mechanism, Environ 516 Prog Sustain Energy 40 (2021). https://doi.org/10.1002/ep.13702. 517 O. Chen, Y. Hao, Z. Song, M. Liu, D. Chen, B. Zhu, J. Chen, Z. Chen, Optimization of 518 [35] 519 photocatalytic degradation conditions and toxicity assessment of norfloxacin under visible light by new lamellar structure magnetic ZnO/g-C3N4, Ecotoxicol Environ Saf 225 (2021). 520 https://doi.org/10.1016/j.ecoenv.2021.112742. 521 522

### **Annexure Tables:**

525526

# Annexure Table 1 - Comprehensive review of photocatalyst, light source, catalyst used, running time, measure of degradation and application

Photocatalyst material	Catalyst preparation	UV Light sources	Application	Removal Efficiency	Optimal dopant percentage	Reaction time	Measure of degradation	Reference
BV loaded rare earth mat RE=Ho, Sm, Yb, Eu, Gd, Nd, Ce and La)	Bismuth Nitrate Pentahydrate, Ammonium Vanadate, Nitric Acid; doping by rare earth oxide	visible light - two 150W tungsten halogen lamps (lambda > 400 nm)	decolorization of methylene blue (MB) under visible light irradiation	80%	Gd 8%	-	measuring the absorbance at 664 nm with UV–vis spectrometry.	[11]
Gd-BV	Bismuth Nitrate Pentahydrate,	sunlight	Rhodamine B	96%	Gd 10%	120 min	UV absorbance spectra and TOC	[12]

	Ammonium						(Total Organic	
	Vanadate, Gd						Compounds)	
	Nitrate					10,		
	Bismuth	metal halide				7//		
	Nitrate,	lamp (400 W)					spectrophotometric	
	Ammonium		removing		15		colorimetric DPC	
La, Gd doped	Vanadate,	was used to	aqueous Cr(VI)	91%		-	method by	[13]
BV	BV HNO <sub>3</sub> ,	simulate	and azo dye				using a UV–vis	
	La Nitrate and	sunlight					spectrophotometer	
	Gd Nitrate	(380–800 nm)						
	Bismuth		Real urban			Diclofenac		
	Nitrate		wastewater.			120 min;		
			Removal of			·	Total Organic	
Gd-BV	Pentahydrate,	UVA-LED	pharmaceutically	80-100%	4% Gd	acetaminophen	Carbon (TOC)	[14]
	Ammonium		active			and	measurements	
	Vanadate, Gd		compounds			azithromycin		
	chloride		(PhACs) and			180 min;		

			bacteria inactivation from urban wastewater effluents; diclofenac, paracetamol, ibuprofen etc					
Gd-BV	Bismuth Nitrate Pentahydrate, Ammonium Vanadate, Gd chloride	LED visible light; An LED lamp with 36 W power consumption and 730 lm luminous intensity	endocrine; decomposition of bisphenol A, bisphenol S and bisphenol AF in water	77%	4% Gd	-	high-performance liquid chromatography (HPLC) equipped with a UV-Vis detector at a wavelength of 270 and 240 nm	[17]

Gd-BV; rGO/Gd/BiVO <sub>4</sub> composite	Bismuth Nitrate Pentahydrate, Ammonium Vanadate, Gd Nitrate, Graphite Oxide	150 W  Xenon lampbased solar simulator. The light intensity was calibrated using a silicon reference cell	photodegradation of Methylene Blue (MB) dye	96.8%			double beam UV– vis spectrophotometer	[22]
Gd-BV		sunlight; at sub-100 °C and enhanced sunlight-driven	organic contaminants removal; ofloxacin (OFL) removal; diclofenac, tetracycline HCl, ofloxacin,	93.14% / 97.98%	5% Gd	-	-	[15]

			rhodamine B, and sulfadiazine					
					,			
			degradation of					
Gd Y co-		sunlight	methylene blue	94%		90 min	uv spectra	[18]
doping BV			dye					
Gd Mo doped	conventional		Site doping					[21] [10]
BV	sintering		analysis		-	-	-	[21] [19]

Parameter and	Parameter	Parameter	Parameter and	Parameter and	Reference
range	and range	and range	range	range	Reference
initial	22.1	no lestico o III		(15	
metformin	GO dosage (50–150 mg L <sup>-</sup>	solution pH (4.5–8.5)		temperature (15 °C–45 °C)	[28]
concentration	1)				[20]
(300–700 mg L <sup>-1</sup> )					
IICl	enzyme		ultrasonication	S. cerevisiae	
HCl concentration (1–3% v/v)	concentration	-	time (5–15	inoculum size	[29]
(1 370 777)	(10–30 U/mL)		min)	(10–20 g/L)	
the initial	TiO <sub>2</sub>				
concentrations of	dosage (250–	initial pH (3–	reaction time	_	[9]
contaminants (10–	1250 mg L <sup>-1</sup> )	11)	(30–150 min)		[>]
50 mg L <sup>-1</sup> )					
	adsorbent				
initial concentration (50	dosage (2 – 4 mg L <sup>-1</sup> ),	рН (6 - 10)	-	temperature (30 – 40°C)	[30]
- 100 μg/L)				- <del>10</del> C)	
	catalyst amount (20– 100 mg)	рН (2.5–6.5)	time (1–30 min)	-	[31]
	100 mg)				

initial ammonia concentration (85– 850 mg L <sup>-1</sup> )	catalyst dosage (0.5–2 g/L)	pH (4–12)	-	-	[32]
initial concentration (10– 200 mg L <sup>-1</sup> )	dose nanoparticles (0.2–0.25 g/L)	pH (3–11)	reaction time (15–120 min)	intensity of UV radiation (8–40 W)	[33]
pollutant concentration (x <sub>1</sub> )  10-100 mg L <sup>-1</sup>	ZnO dose (x <sub>3</sub> ) 0.05-0.75 g/L	-	irradiation time (x <sub>2</sub> ) 30-90 min	stirring speed (x <sub>4</sub> ) 100-600 rpm	[34]
norfloxacin  concentration (3–  15 mg L <sup>-1</sup> )	photocatalyst concentration (0.2–1.8 g/L)	solution pH (4- 12)		-	[35]

## Annexure Table 3 – Fit summary

Source	Sequential p-value	Adjusted R <sup>2</sup>	Predicted R <sup>2</sup>	Prediction
Linear	< 0.0001	0.8296	0.7869	
2FI	0.9959	0.7799	0.6019	
Quadratic	< 0.0001	0.9953	0.9866	Suggested
Cubic	0.7097	0.9942	0.8225	Aliased

